Density functional theory study on the initial reactions of d-Xylose and d-Xylulose dehydration to furfural

Fang, Xiaowei; Andersson, Martin P; Wang, Ze; Song, Wenli; Li, Songgeng

Published in:
Carbohydrate Research

Link to article, DOI:
10.1016/j.carres.2021.108463

Publication date:
2022

Document Version
Publisher's PDF, also known as Version of record

Carbohydrate Research 511 (2022) 108463

Contents lists available at ScienceDirect

Carbohydrate Research

journal homepage: www.elsevier.com/locate/carres

Density functional theory study on the initial reactions of D-Xylose and D-Xylulose dehydration to furfural

Xiaowei Fang [a,b], Martin P. Andersson [c,*], Ze Wang [b,**], Wenli Song [b], Songgeng Li [b]

[a] Xi'an Thermal Power Research Institute Co, LTD, China
[b] State Key Laboratory of Multi-Phase Complex Systems, Institute of Process Engineering, Chinese Academy of Sciences, Sino-Danish College, University of Chinese Academy of Sciences, Sino-Danish Center for Education and Research, Beijing, 100190, China
[c] Department of Chemical and Biochemical Engineering, Technical University of Denmark, 2800, Lyngby, Kgs, Denmark

ARTICLE INFO

Keywords:
Reaction mechanisms
Kinetic model
Energy barriers
Rate-limiting step
Dominant reaction pathway

ABSTRACT

The mechanism of the initial reactions in the acid-catalytic conversion of D-xylose/D-xylulose to furfural was studied with density functional theory. The reactions included mutual transformations among D-xylose, D-xylulose and the intermediate of 1,2-enediol. The catalytic performances of several acids including H_2SO_4, HNO_3, HCl, HBr and HI, and the solvent effects of water and THF (tetrahydrofuran) were studied. A simplified kinetic model of the D-xylose/D-xylulose-to-furfural conversion in water solvent was built, with the assumption that the conversion from 1,2-enediol to furfural was the rate-limiting step and could be treated as one-step reaction. The simulation can well fit the experimental regulation, which verifies the rationality of the model simplification. The dominant reaction pathways from D-xylose/D-xylulose to furfural were deduced based on the calculated energy barriers and corresponding reaction rate constants, with different acid catalysis and reaction mediums.

1. Introduction

Furfural is a promising platform chemical that can be employed to produce higher value C_4 and C_5 chemicals and long-chained biofuel [1–4]. Furfural is mainly produced from acid-catalyzed dehydration of pentosans derived from lignocellulosic biomass [5]. D-xylose-to-furfural conversion in homogenous acidic aqueous solution is a classic reaction route in furfural production. A deep understanding on this reaction mechanism would help the establishment of a kinetic model and further development of industrial production.

More than one mechanism of D-xylose-to-furfural conversion over homogenous acid in aqueous solution have been reported in different studies, under the different reaction systems. As early as 1932, Hurd et al. proposed a reaction mechanism via an 2,3-unsaturated aldehyde followed by the intermolecular dehydration to form a 5-membered ring and then dehydration to furfural in the acidic solution (Scheme S1) [6]. This mechanism conformed to the well-known reaction in organic chemistry that β-elimination reaction took place very readily to lose water molecule on β-hydroxyaldehydes. Another reaction mechanism was suggested to follow a ring-opening process via a 1,2-enediol intermediate formation and subsequent dehydration to furfural (Scheme S2) [7–10]. The process started with the acyclic form of the D-xylose, which then isomerized and dehydrated to generate furfural. Also, a cyclic reaction mechanism was proposed that the reaction started with the pyranose form of D-xylose, followed by the direct intramolecular rearrangement via the protonation on O-2 of the pyranose ring leading to the 2,5-anhydroxylose intermediate formation. Then furfural could be obtained by the subsequent dehydration of the 2,5-anhydroxylose (Scheme S3) [9,11,12].

Some isotope exchange experiments were conducted to test the validity of the proposed mechanisms by the reaction of labeled model compounds. Bonner et al. prepared D-xylose-1-^{14}C and decomposed in 12% HCl aqueous solution. It was found that the labeled carbon at C-1 position was almost fully transferred to the 'aldehydic' carbon of the product, 2-furaldehyde-α-^{14}C [13]. Feather et al. used a similar isotope-exchange technique of the conversion of D-xylose to 2-furaldehyde in the acidified, tritiated water. It was found that 2-furaldehyde had essentially no carbon-bound tritium, indicating that no solvent hydrogen was incorporated into the product during the reaction [8]. Another evidence was presented for an intramolecular hydrogen-transfer (hydride shift) from C-2 to C-1 during the direct conversion of D-glucose-2-^{3}H into D-fructose-1-^{3}H in 1 mol/L H_2SO_4 acid

* Corresponding author.
** Corresponding author.
E-mail addresses: martan@kt.dtu.dk (M.P. Andersson), wangze@ipe.ac.cn (Z. Wang).

https://doi.org/10.1016/j.carres.2021.108463
Received 23 June 2021; Received in revised form 19 October 2021; Accepted 22 October 2021
Available online 29 October 2021

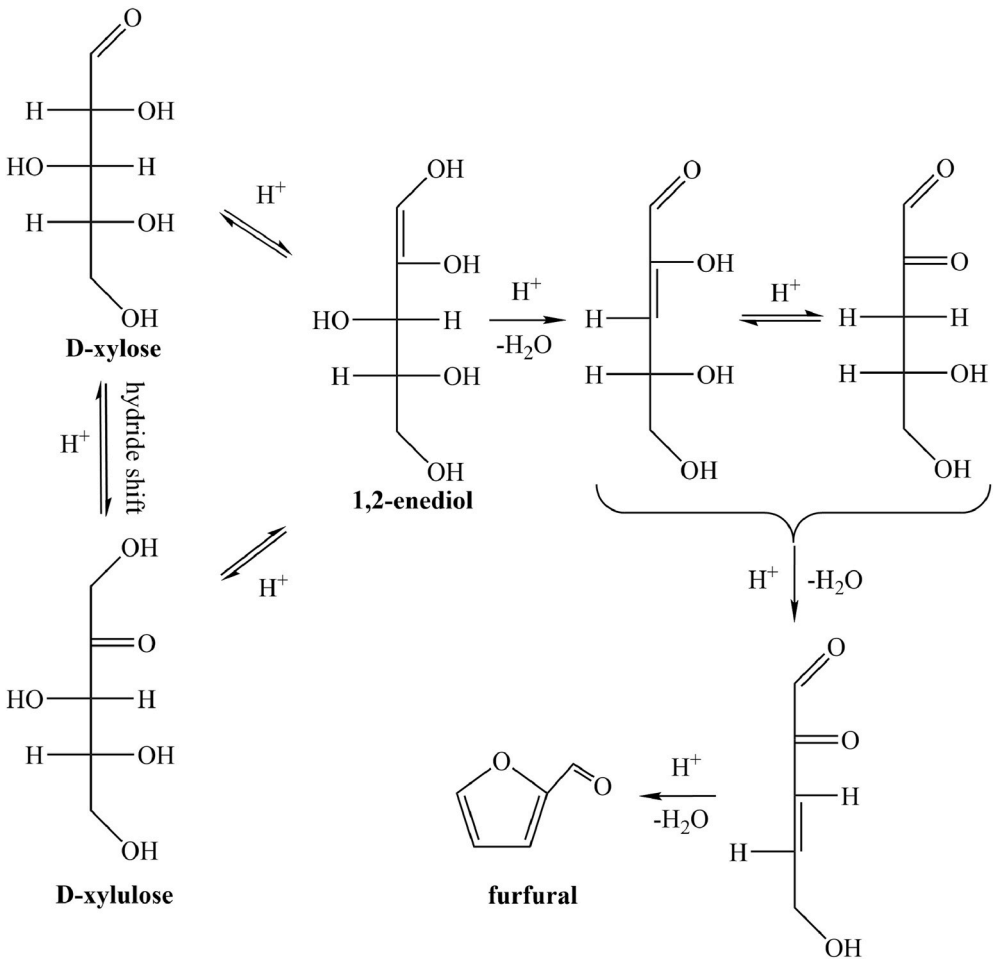

Scheme 1. Putative reaction mechanism for D-xylose-to-furfural conversion.

solution [14]. Danon et al. also extended such hydride shift to the D-xylose and D-xylulose when using homogenous acid as catalyst (Scheme S4), due to the similarity between glucose and xylose [15]. Besides, Blinder et al. reported a similar conclusion that the transfer of the deuterium label from C-2 to C-1 was consistent with the hydride shift during the chromium(III)-catalyzed conversion of D-xylose to furfural [16].

These observations, the transfer of the labeled carbon on D-xylose-1-^{14}C to 2-furaldehyde-α-^{14}C and the absence of solvent hydrogen in furfural, supported all the foregoing mechanisms. However, these three proposed mechanisms failed to explain the hydride shift because the product from a hydride shift, D-xylulose, was not involved in the mechanism. Compared to the other two mechanisms, this mechanism proposed a key intermediate: 1,2-enediol intermediate, which allowed for D-xylose-to-D-xylulose (aldose-to-ketose) isomerization through two-step enolizations. The other two mechanisms could not explain the production of D-xylulose.

To better explain the experimental results, we modelled an acyclic reaction mechanism under homogenous acidic catalysis, including D-xylose-to-D-xylulose isomerization by both hydride shift and enolization, followed by the dehydration of 1,2-enediol intermediate to furfural (Scheme 1).

In Scheme 1, the formation of 1,2-enediol intermediate is a precondition of yielding furfural. Since enolization reactions are normally reversible, the formation of 1,2-enediol intermediate is considered as the rate limiting step in the furfural production under acidic conditions [15,17,18]. Thus, the mutual transformation among D-xylose, 1,2-enediol and D-xylulose should be studied with emphasis in furfural production.

In this paper, the energetics of the mutual transformation processes were modelled using density functional theory in the presence of several strong acids, including H_2SO_4, HNO_3, HCl, HBr and HI. Furthermore, based on the assumption of 1,2-enediol formation being the rate limiting step, the formation of furfural from 1,2-enediol was simplified as one-step reaction, and a simplified kinetic model to produce furfural was set up. The reasonableness of the simplification was verified by comparing the kinetic model results with reported experimental data. The solvent effect of THF (tetrahydrofuran) was also studied, and the dominant reaction pathway for furfural formation was determined with different acid catalysts.

1.1. Computational approach

The density functional theory calculations were performed using Gaussian 09 [19–24]. All calculations were performed using the B3LYP functional [21,25–27] and the SMD model of water or THF (tetrahydrofuran) solvent [28], and the reaction condition was set at a temperature of 463 K and a pressure of 1 atm [18].

The computations including optimization, frequency analysis and intrinsic reaction coordinate (IRC) calculation were conducted at the same computational level [28]. And for the calculation with H_2SO_4, HNO_3, HCl and HBr acids, 6-31G(d) basis set was applied while Lanl2DZ basis set was employed for the calculation with HI acid [29]. The energy minima were confirmed by the absence of imaginary frequencies. Transition states (TS) were verified by the presence of single imaginary frequency. IRC calculation based on the optimized TS were carried out to confirm that TS connected with reactants and products. Besides the

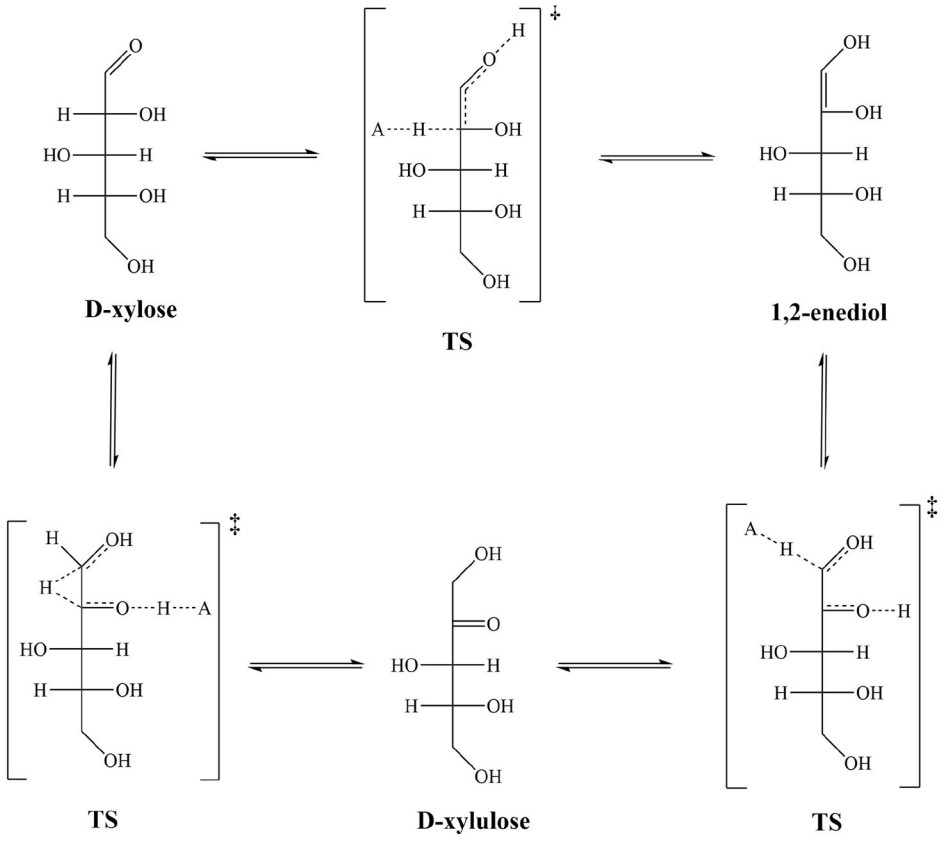

Scheme 2. The structures of TS in the mutual transformations among D-xylose, 1,2-enediol and D-xylulose.

bonding-state species were obtained by optimizing the searched structures at the two end sides of reaction coordinates from IRC calculation. Higher computational levels were used for electronic energy calculations of all species to get more accurate energies. The calculations involving the elements of C, H, O, S, N, Cl were conducted at the basis set of 6–311++G(d,p) while def2-TZVP basis set was applied to calculate the elements of Br and I [28–30]. Def2-TZVP was transferred from Turbomole 7.3 by Basis Set Exchange [31,32].

In the calculations, there are seven reaction coordinates for describing the energetics of each reaction step:

(1) separated reactant and non-dissociated acid (HA), denoted as: reactant + HA
(2) separated reactant, H^+ and corresponding anion (A^-), denoted as: reactant + H^+ + A^-
(3) H^+ and the reactant bonded to A^-, denoted as: reactant - H^+ - A^-
(4) the transition state, denoted as: TS
(5) H^+ and the product bonded to A^-, denoted as: product - H^+ - A^-
(6) separated product, H^+ and corresponding anion (A^-), denoted as: product + H^+ + A^-
(7) separated product and non-dissociated acid (HA), denoted as: product + HA

The Gibbs free energies of all species were obtained by the sum of electronic energies and thermal corrections to Gibbs free energies. The electronic energies were calculated at SMD-B3LYP/6-311++G(d,p) (for C, H, O, S, N, Cl elements) or SMD-B3LYP/def2-TZVP (for Br and I elements) level, and the values of thermal corrections to Gibbs free energies were obtained from frequency analysis at the levels of SMD-B3LYP/6-31G(d) and SMD-B3LYP/Lanl2DZ respectively. The detailed calculation can be expressed by eqn (1):

$$G(T) = \varepsilon_0 + G_{corr}(T) \quad (1)$$

where $G(T)$ represented the absolute Gibbs free energy at T = 463 K, in kcal/mol; ε_0 was the electronic energy, in kcal/mol; $G_{corr}(T)$ represented the thermal correction to Gibbs free energy, in kcal/mol, which could be obtained from frequency analysis.

The establishment of microkinetic model required to solve the reaction rate constant for each elementary reaction, which could be determined by the following Eyring equation [21]:

$$k = \frac{\kappa k_B T}{h} e^{-\frac{\Delta G^{\ddagger}}{RT}} \left(M^{1-m}\right) \quad (2)$$

where κ was the transmission coefficient, taken to be 1; k_B was the Boltzmann constant, 1.381×10^{-23} J/K; T was the temperature, 463 K; h was the Plank's constant, 6.626×10^{-34} J·s; $\Delta G^{\ddagger}$ was the Gibbs free energy of activation (energy barrier); R was the gas constant, 1.987 cal/mol/K; M was the molarity; m was the molecularity of the reaction, taken to be 1.

2. Results and discussion

2.1. Energy barriers for mutual transformations in water

The determination of Gibbs free energy in reaction process is crucial for the calculation of energy barriers. To decrease the effects from the inaccurate calculation of absolute Gibbs free energy for charged H^+ and A^- ions, especially for H^+ ion which has no electron, the sum of the Gibbs free energies of H^+ and A^- at 463 K was solved by the Gibbs free energy change of acid dissociation ($\Delta G_a(463\,K)$) plus the Gibbs free energy of the non-dissociated acid (HA). The Gibbs free energy calculation for the uncharged acid (HA) is much more accurate and reliable.

Typically, ΔG_a can be obtained using dissociation constant of HA acid (pK_a), as shown in eqn (3) [28,33], however pK_a values are merely available in water at 298 K. Thus $\Delta G_a(463\,K)$ required to be further

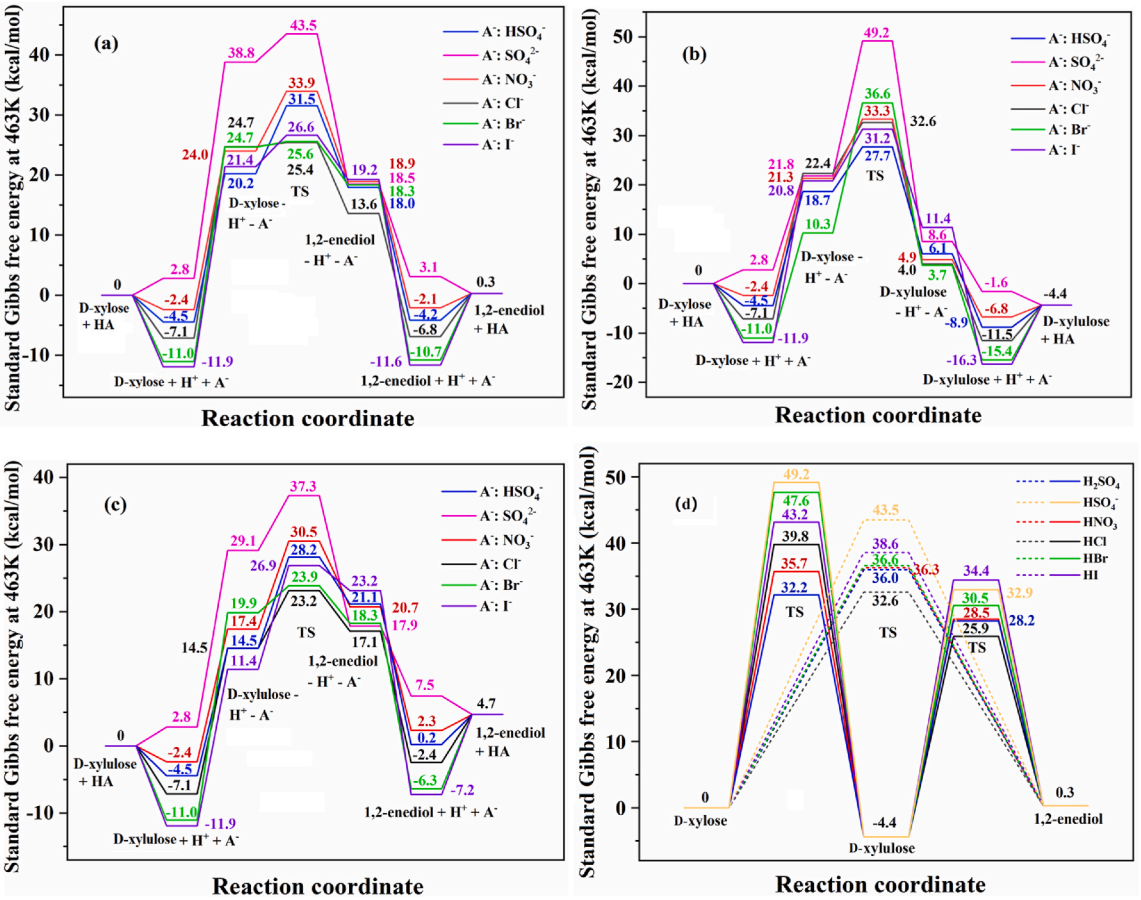

Fig. 1. Standard Gibbs free energy profile for the mutual transformations over different acids in water at 463 K. (a) between D-xylose and 1,2-enediol; (b) between D-xylose and D-xylulose; (c) between D-xylulose and 1,2-enediol. (d) concise standard Gibbs free energy in the mutual transformations. The ionized anion is denoted as A^-.

solved by eqn (4) [34]. In eqn (4), the first term on the right side is the aqueous-phase Gibbs free energy of acid dissociation at 298 K, it is calculated by eqn (3), the pK_a values are from references (Table S1) [35,36]. The second and third terms are obtained by the calculation of Gibbs free energy on individual compounds in chemical eqn (5). The calculation results of $\Delta G_a(463\,K)$ for different acids are also presented in Table S1.

$$\Delta G_a = 2.303RT\Delta pK_a \tag{3}$$

$$\Delta G_a(463\,K) = \Delta G_a(aq, 298\,K)_{ref} + \Delta G_a(463\,K)_{calc} - \Delta G_a(aq, 298\,K)_{calc} \tag{4}$$

$$HA(aq) + H_2O(l) \rightarrow H_3O^+(aq) + A^-(aq) \tag{5}$$

The Gibbs free energy of charged H^+ and A^- ions in water can be calculated by the approach above. In addition, we used the relative difference of the Gibbs free energy for calculating charged ions instead of their absolute values, avoiding the inaccuracy of absolute values for calculating charged ions.

Scheme 2 displays the optimized structures of TS in the mutual transformations among D-xylose, 1,2-enediol and D-xylulose under the catalysis of different acids including H_2SO_4, HNO_3, HCl, HBr and HI. TS are formed by anions attacking the hydrogen atoms on the reactant molecule to form electron-rich carbon or oxygen atoms, which would capture the hydrogen ions. Fig. 1 shows the Gibbs free energy changes for the mutual transformations among D-xylose, 1,2-enediol and D-xylulose in water at 463 K, and the Gibbs free energy change of acid dissociation at 463 K. It is found that $\Delta G_a(463\,K) < 0$ for all the acid dissociation processes except the second dissociation of H_2SO_4. As could be expected of strong acids in water, the free energy of separated reactant, H^+ and corresponding anion (compound + H^+ + A^-) are always lower than that of the non-dissociated acid (compound - HA).

The standard Gibbs free energy at 463 K of "D-xylose + HA" is set as zero. The condensed energy barriers both for forward and reverse reactions are further shown in Fig. 1 (d). A higher energy barrier is obtained when SO_4^{2-} catalyzes the mutual transformations compared to that of HSO_4^-, which means that the second dissociation of H_2SO_4 acid contributes little to the overall transformations. For the transformation from D-xylose to 1,2-enediol, the energy barriers for different acids can be ranked as: HCl < H_2SO_4 < HNO_3 < HBr < HI; For the transformation from D-xylose to D-xylulose, it can be ranked as:H_2SO_4 < HNO_3 < HCl < HI < HBr. For the transformation from D-xylulose to 1,2-enediol, it can be ranked as: HCl < H_2SO_4 < HNO_3 < HBr < HI. For all acids calculated in Fig. 1 (d), the 1,2-enediol intermediates are more readily transferred to D-xylulose rather than D-xylose due to the lower energy barriers, which means that the 1,2-enediol intermediate formed from D-xylose is almost irreversible, because the transformation from 1,2-enediol to D-xylulose has lower energy barrier than to D-xylose. Thus, it is more likely to achieve equilibrium between 1,2-enediol and D-xylulose. This conclusion explains the experimental phenomena well that 1,2-enediol intermediate to be irreversibly formed from the aldopentose in acidic conditions, showing a partial equilibration with keto form [18,37].

The best acid in catalyzing the transformation between D-xylose and 1,2-enediol is HCl, between D-xylose and D-xylulose it is H_2SO_4, and between D-xylulose and 1,2-enediol it is HCl. The length change of relevant bonds in the transformations is shown in Fig. 2. The structures shown in Fig. 2 are the bonded states or TS. It is found that the H atom between Cl atom and C atom in TS moves back and forth in the

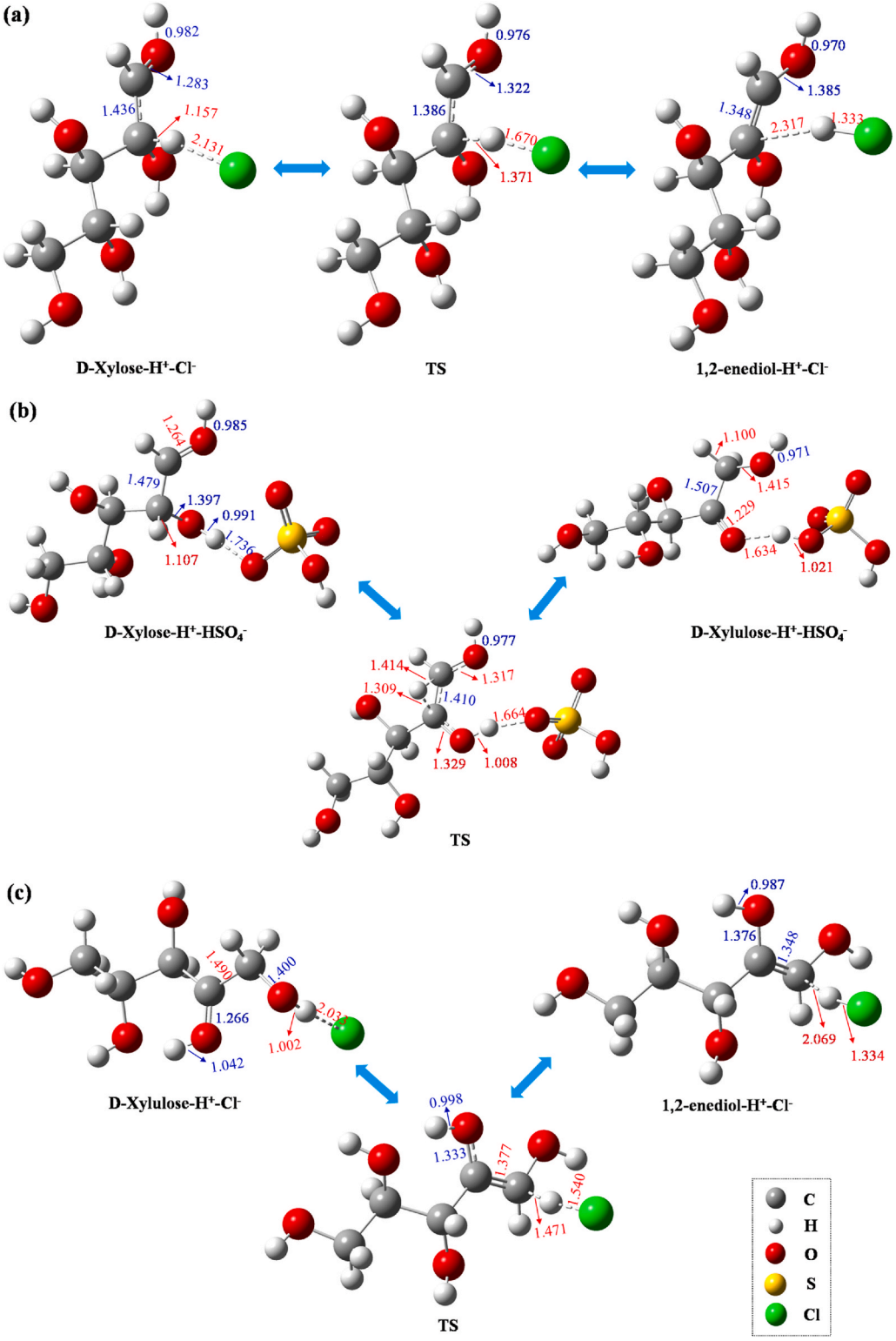

Fig. 2. The bond length changes in the mutual transformation of D-xylose, 1,2-enediol and D-xylulose (a) the transformation between D-xylose and 1,2-enediol under HCl catalysis; (b) the transformation between D-xylose and D-xylulose under H_2SO_4 catalysis; (c) the transformation between D-xylulose and 1,2-enediol under HCl catalysis.

transformation from D-xylose or D-xylulose to 1,2-enediol, as shown in Fig. 2 (a) and (c). It causes the change of the unsaturation degree of the C atom, and then forms the C=C double bond and the enol structures. In addition, the bond length of the C=O double bond (carbonyl group) in the bonded state continues to increase until it turns to the C-O single bond. The C-C single bond between C-1 and C-2 position continues to shorten until it becomes a C=C double bond. The transformation from D-xylose to D-xylulose is shown in Fig. 2 (b). It is found that the H atom between C-1 and C-2 position in TS moves back and forth, giving rise to the change of the unsaturation degree of the C atom, and then forms the carbonyl structures. The bond length of the C=O double bond (carbonyl group) in the bonded state keeps increasing until it becomes a C-O single

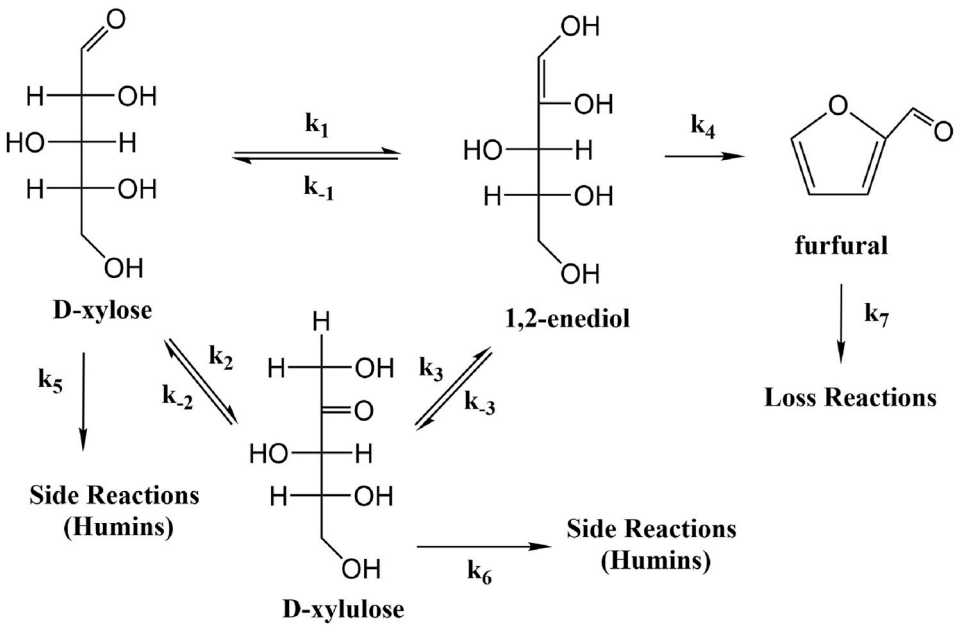

Scheme 3. The simplified reaction mechanisms for D-xylose/D-xylulose-to-furfural conversion.

bond, while the C-C single bond between the C-1 and C-2 position first shortens and then increases.

In addition, G. Marcotullio reported the effect of adding Cl^-, Br^-, I^- ions to the H_2SO_4 acid-catalyzed D-xylose -to-furfural reaction system, it was found that the formation of 1,2-enediol from D-xylose was promoted with the order: $Cl^- > Br^- > I^-$ [17]. It is consistent with our results shown in Fig. 1 (d). The supplementary Cl^-, Br^-, I^- ions coupling with the H^+ ions from the second dissociation of H_2SO_4 forms corresponding acid of HCl, HBr and HI, these acids can be used to accelerate the conversion of D-xylose -to-1,2-enediol and of D-xylulose -to-1,2-enediol with the order: HCl > HBr > HI, though their effects on D-xylose -to- D-xylulose conversion are limited.

2.2. Simplified kinetic model for D-xylose/D-xylulose-to-furfural conversion in water

O. Ershova et al. concluded that the D-xylose isomerization to D-xylulose with subsequent furfural formation is not a primary reaction pathway by mechanistic modeling study. It stated that the D-xylulose as a key intermediate for furfural production from D-xylose was rejected, and the primary reaction route involved another short-living intermediate that reacted rapidly to the furfural [5]. Gianluca et al. confirmed that the key intermediate was 1,2-enediol, which could equilibrate with both D-xylose and D-xylulose, and the formation of 1,2-enediol as the rate-limiting step could further react to form furfural with the presence of acid [18].

Based on the mutual transformations among D-xylose, 1,2-enediol and D-xylulose, a simplified reaction mechanism can be set up to describe the D-xylose/D-xylulose-to-furfural conversion in water, as shown in Scheme 3. For the D-xylose/D-xylulose-to-furfural conversion under acidic catalysis, the formation of 1,2-enediol is considered as the rate limiting step. Thus, we briefly describe the furfural formation by direct conversion of 1,2-enediol. Besides, the side reactions of D-xylose, D-xylulose and furfural are inevitable in the experiments, which readily form unidentifiable humin-like polymers [15,38,39].

Acid concentration has a significant effect on the D-xylose/D-xylulose decomposition and furfural formation [15]. Besides, the mechanism of furfural formation goes beyond the proton catalysis, also dependent on the type of anions [40]. The kinetic model should reflect the influence from both H^+ ions and anions. It needs to be embodied at two aspects: one is the different energy barriers resulted from changing anions type; another one is the acid concentration. Eyring equation (2) is merely dependence on the energy barrier, $\Delta G^{\ddagger}$, thus it should multiply by the acid concentration for the determination of reaction rate constants. As shown in Scheme 3, every reaction step follows a first-order reaction [5,15,18]. The detailed concentration evolutions of D-xylose, D-xylulose, 1,2-enediol and furfural can be expressed as the following differential equations (6)~(9).

$$-\frac{dc_{D-xylose}}{dt} = (k_1 + k_2 + k_5)c_{D-xylose} - k_{-1}c_{1,2-enediol} - k_{-2}c_{D-xylulose} \quad (6)$$

$$\frac{dc_{D-xylulose}}{dt} = k_2 c_{D-xylose} + k_{-3}c_{1,2-enediol} - (k_{-2} + k_3 + k_6)c_{D-xylulose} \quad (7)$$

$$\frac{dc_{1,2-enediol}}{dt} = k_1 c_{D-xylose} + k_3 c_{D-xylulose} - (k_{-1} + k_{-3} + k_4)c_{1,2-enediol} \quad (8)$$

$$\frac{dc_{furfural}}{dt} = k_4 c_{1,2-enediol} - k_7 c_{furfural} \quad (9)$$

In the literature, HCl and H_2SO_4 acids are reported to be the most used and efficient homogenous catalysts for the production of furfural from D-xylose/D-xylulose in water [18,40,41]. Thus HCl and H_2SO_4 acids are employed in the kinetic model to compare the results with experimental data. The reaction conditions in our model was set as: reaction temperature of 190 °C, acid concentration of 0.1 mol/L, and D-xylose/D-xylulose dosage of 0.05 mol, these reaction conditions are readily to offer high conversion of reactant and high yield of furfural [5,18,42]. The produced H^+ and SO_4^{2-} from second dissociation of H_2SO_4 acid has much weaker catalytic ability for the mutual transformations compared to that of H^+ and HSO_4^- dissociated from the first dissociation of H_2SO_4 acid. Based on the obtained $\Delta G_a(463\,K)$ of the second dissociation of H_2SO_4 acid (Table S1), we can calculate and know that 28% of HSO_4^- ions dissociate into H^+ and SO_4^{2-} ions when use 0.1 mol/L H_2SO_4 acids, then we get 128% H^+ ions concentration (0.128 mol/L) and 72% HSO_4^- ions concentration (0.072 mol/L), thus the effective concentration of H_2SO_4 acid can be calculated as 128% × 72% = 92%, namely, the effective concentration of H_2SO_4 acid in this reaction system is 0.092 mol/L.

It is hard to study the formation of humin-like polymers using transition state theory. The referenced values for k_5, k_6, k_7 are from

Table 1
The adopted values for k_5/k_1, k_6/k_3, k_7/k_1, and the equivalent energy barriers for the side reactions [5,18].

Acid	HCl	H_2SO_4
k_5/k_1	0.287	0.520
k_6/k_3	0.677	0.677
k_7/k_1	0.058	0.065
$\triangle G^{\ddagger}_5$ (kcal/mol)	33.7	36.6
$\triangle G^{\ddagger}_6$ (kcal/mol)	26.3	28.6
$\triangle G^{\ddagger}_7$ (kcal/mol)	35.2	38.5

literatures which have similar reaction conditions to present how much reactants or products would react to produce by-products. Specifically, the values of k_5, k_6, k_7 are determined based on the same ratios of k_5/k_1, k_6/k_3, k_7/k_1 to literatures (see Table S2). Since we lack the referenced kinetic data of the D-xylose-to-D-xylulose hydride shift and D-xylulose-to-1,2-enediol enolization under HCl acid catalysis, only referenced values of k_1 and k_3 are applied. The ratio of k_6/k_3 for HCl acid is unknown and we therefore assume it to be the same as that for H_2SO_4 acid catalysis. The adopted values for k_5/k_1, k_6/k_3, k_7/k_1, and the equivalent energy barriers are presented in Table 1.

The differential equations can be solved based on the formation of 1,2-enediol as rate limiting step, even if the k_4 value is unknown. We have used two strategies. The first assumption is $\frac{dc_{1,2-enediol}}{dt} = 0$ because 1,2-enediol is in steady state [18]. The second method was to specify an energy barrier for the 1,2-enediol-to-furfural conversion, which was smaller than any energy barriers related to the formation of 1,2-enediol, to assure the reactions proceeding along the direction of furfural formation, namely $\triangle G^{\ddagger}_4 < \triangle G^{\ddagger}_{-3}$. The results of the two strategies are compared and no essentially difference are found (see Fig. S1~S4), which means that the steady state of 1,2-enediol is a reasonable inference to solve the differential equations. Based on the first strategy, the reactant conversion evolution of D-xylose or D-xylulose and the product yield evolution of furfural under HCl or H_2SO_4 acids catalysis at 463 K in water are shown in Fig. 3.

O. Ershova et al. reported that similar furfural yields were observed in the 0.1 mol/L H_2SO_4 acid-catalyzed conversion when respectively using D-xylose and D-xylulose as reactant at the temperature from 453 K to 493 K. This is in good agreement with the results shown in Fig. 3 (c) and (d). Based on previous reports, D-xylulose reacted much faster to produce furfural in acidic solution compared to that of D-xylose [2]. For example, reaching maximum furfural yield from the conversion of D-xylulose required less time than that from the conversion of D-xylose under 0.1 mol/L HCl acid-catalysis [43]. Likewise, D-xylulose was also reported to react faster than D-xylose for the production of furfural under 0.1 mol/L H2SO4 acid catalysis (Fig. S5) [5]. These phenomena are analogous to the lower reactivity of glucose than fructose for the formation of HMF [44,45]. And this is in good agreement with our modeling under HCl or H_2SO_4 acid catalysis, as shown in Fig. 3 (a)–(d). In our model, D-xylulose has a better reactivity to form furfural than that of D-xylose when using HCl or H_2SO_4. Gianluca et al. reported that HCl acid achieved a higher furfural yield than H_2SO_4 in D-xylose-to-furfural conversion at similar reaction condition of 200 °C and 0.05 mol/L acid

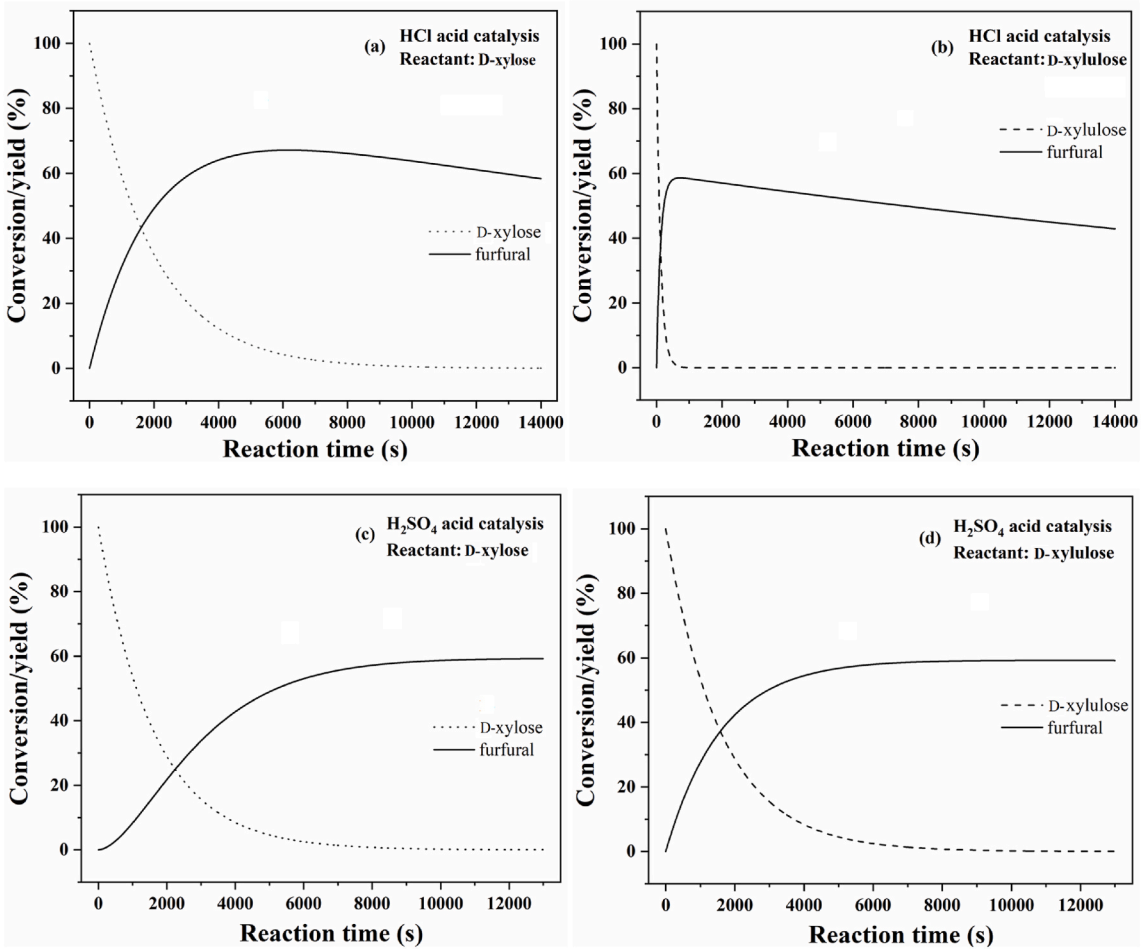

Fig. 3. The reactant conversion evolution of D-xylose or D-xylulose, and the product yield evolution of furfural under 0.1 mol/L HCl or H_2SO_4 acids catalysis at 463 K in water. (a) D-xylose-to-furfural conversion under HCl catalysis; (b) D-xylulose-to-furfural conversion under HCl catalysis; (c) D-xylose-to-furfural conversion under H_2SO_4 catalysis; (d) D-xylulose-to-furfural conversion under H_2SO_4 catalysis.

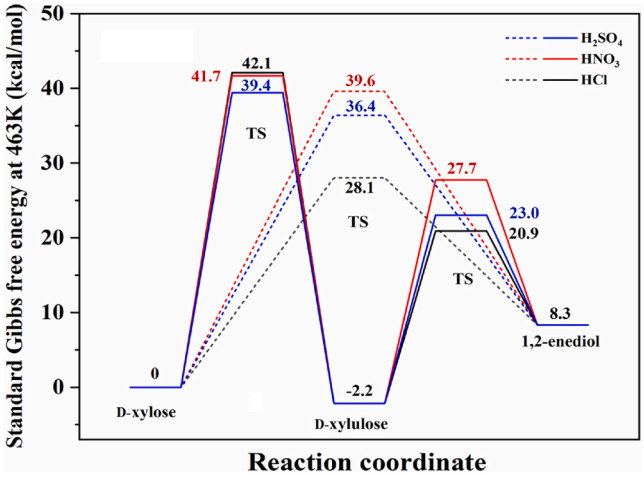

Fig. 4. Concise Standard Gibbs free energy in the mutual transformation among D-xylose, 1,2-endiol and D-xylulose over different acids (H_2SO_4, HNO_3 or HCl) at 463 K in THF.

concentration (Fig. S6) [18], which is also consistent with our calculations, as seen in Fig. 3 (a) and (c). In summary, the results of the kinetic model are in good agreement with the experimental rules reported in the literature, and the simplification that furfural is directly generated from the 1,2-enediol is proved to be very reasonable.

In the kinetic model, the concentrations of HCl and H_2SO_4 acid are same (0.1 mol/L), but the reaction routes (energy barriers of the D-xylose-D-xylulose-1,2-enediol conversion) are quite different, as shown in Fig. 1. Additionally, the concentration of H^+ in H_2SO_4 catalytic system (0.128 mol/L) is higher than that in HCl system (0.1 mol/L), because there is one more step of H^+ dissociation from H_2SO_4 than that from HCl, but in the reaction from D-xylose to 1,2-enediol and in the reaction from D-xylulose to 1,2-enediol, the catalytic effect of HCl is even stronger than that of H_2SO_4. It indicates that the reaction is not only related with the concentration of H^+ (acid catalysis) but also the type of anion (anion catalysis). The speculation can be verified from the combination of anion (Cl^- or SO_4^{2-}) with reactant (D-xylose or D-xylulose) in the transition state, as Fig. 2 illustrated.

2.3. The mutual transformations among D-xylose, D-xylulose and 1,2-enediol in THF

THF (tetrahydrofuran) as a biomass-derived aprotic polar solvent is extensively applied in biomass conversion. It is favorable to the formation of desired products including HMF and furfural [46–50]. Thus the mutual transformations in THF are also studied to reveal the reaction mechanism and to offer theoretical guidance to the further experiment researches.

The acid dissociation processes in THF can be expressed as chemical eqn (10). The Gibbs free energy change of acid dissociation in THF can be solved by the same approach as that in water (Table S3).

$$HA(THF) + THF\ (l) \rightarrow THF \cdot H^+(THF) + A^-(THF) \quad (10)$$

The energy barriers of the mutual transformations among D-xylose, D-xylulose and 1,2-enediol over different acids in THF at 463 K are presented in Fig. 4. In Fig. 4, we focus on investigating the most interesting acids in industry, H_2SO_4, HNO_3 and HCl acid. The detailed energy variation can be found in Fig. S7. The combination of H^+ and SO_4^{2-} performs even worse in catalyzing the mutual transformations in THF, thus the catalysis over H_2SO_4 acid shown in Fig. 4 is from the effect of H^+ and HSO_4^-.

Comparing Figs. 4–1(d), it is found that D-xylulose is still the most stable compound in THF while 1,2-enediol becomes more unstable. For the transformation between D-xylose and 1,2-enediol, THF solvent accelerates this process only when using HCl acid for catalysis, compared to that in water. The energy barriers in THF can be ranked as HCl < H_2SO_4 < HNO_3. For the transformation between D-xylose and D-xylulose, THF solvent deteriorates the catalytic performance for all tested acids, and this process is almost intercepted by THF solvent according to the calculation of Eyring equation. For the transformation between D-xylulose and 1,2-enediol, THF solvent accelerates this conversion for all acids and it has lowest energy barriers for all acids compared to other two transformation processes. The energy barriers in THF can be ranked as HCl < H_2SO_4 < HNO_3.

Table 2
Energy barriers and reaction rate constants in different formation route of 1,2-enediol from D-xylose with water or THF as reaction medium.

Reaction medium	Acid	D-xylose-1,2-enediol route		D-xylose-D-xylulose-1,2-enediol route	
		Energy barrier (kcal/mol)	Reaction rate constant, k (h^{-1})	Energy barrier (kcal/mol)	Reaction rate constant, k (h^{-1})
Water	H_2SO_4	36.0	0.35	32.6	14
	HNO_3	36.3	0.25	35.7	0.48
	HCl	32.6	14	39.8	$5.6*10^{-3}$
	HBr	36.6	0.18	47.6	$1.2*10^{-6}$
	HI	38.6	0.020	43.2	$1.4*10^{-4}$
THF	H_2SO_4	36.4	0.23	39.4	$8.6*10^{-3}$
	HNO_3	39.6	$7.0*10^{-3}$	41.7	$7.1*10^{-4}$
	HCl	28.1	1870.62	42.1	$4.58*10^{-4}$

For the D-xylulose-to-furfural conversion, all tested acids have a good performance in the two solvents. THF are the better solvents than water for all acids and HCl acid performs best in all solvents. And HCl acid is the best acid for any solvents to accelerate D-xylose-to-furfural conversion. For H_2SO_4 acid-catalyzed the D-xylose-to-furfural conversion, THF solvent is not a suitable media compared to water since the transformation between D-xylose and D-xylulose is blocked in THF. Thus, for further experimental studies, THF can be a good reaction medium for the D-xylulose-to-furfural conversion. For D-xylose-to-furfural conversion, the mixture of water with THF might be an excellent solvent, the combination of different acids can be together used. For example, employing H_2SO_4 acid promotes the transformation between D-xylose and D-xylulose, at the same time add HCl acid to accelerate the transformation between D-xylose and 1,2-enediol.

2.4. The dominant reaction pathway of furfural formation in different solvents

In D-xylose-to-furfural conversion, there are two formation routes of 1,2-enediol: D-xylose-1,2-enediol route and D-xylose-D-xylulose-1,2-enediol route. Thus, the reaction pathway of D-xylose-to-furfural conversion can be divided into two routes after simplifying the 1,2-enediol-to-furfural conversion as one-step reaction. The first one is D-xylose-1,2-enediol-furfural route; the second one is D-xylose-D-xylulose-1,2-enediol-furfural route. The formation route of 1,2-enediol determines the dominant reaction pathway of D-xylose-to-furfural conversion. Based on the energy changes in the mutual transformations of D-xylose, D-xylulose and 1,2-enediol, the energy barriers and corresponding reaction rate constants of two different formation routes of 1,2-enediol in water or THF solvent can be solved, as presented in Table 2.

In Table 2, when using water as reaction medium, the dominant reaction pathway under H_2SO_4 acid catalysis is D-xylose-D-xylulose-1,2-enediol-furfural route while the dominant reaction pathway under HCl, HBr or HI acid catalysis is D-xylose-1,2-enediol-furfural route. The energy barriers difference between D-xylose-1,2-enediol transformation and D-xylose-D-xylulose-1,2-enediol transformation is small when using HNO_3 acid as catalyst, the reaction rate constant of D-xylose-D-xylulose-1,2-enediol is 1.9 times than D-xylose-1,2-enediol based on the

Table 3
Energy barriers and reaction rate constants in different formation route of 1,2-enediol from D-xylulose with water or THF as reaction medium.

Reaction medium	Acid	D-xylulose-1,2-enediol route		D-xylulose-D-xylose-1,2-enediol route	
		Energy barrier (kcal/mol)	Reaction rate constant, k (h^{-1})	Energy barrier (kcal/mol)	Reaction rate constant, k (h^{-1})
Water	H_2SO_4	32.6	14.03	36.6	0.18
	HNO_3	32.9	10.13	40.1	$4.03*10^{-3}$
	HCl	30.3	171.06	44.2	$4.67*10^{-5}$
	HBr	34.9	1.15	52.0	$9.69*10^{-9}$
	HI	38.8	0.02	47.6	$1.16*10^{-6}$
THF	H_2SO_4	25.2	43787.98	41.6	$7.89*10^{-4}$
	HNO_3	29.9	264.26	43.9	$6.48*10^{-5}$
	HCl	23.1	429504.47	44.3	$4.19*10^{-5}$

calculation of Eyring equation, thus, D-xylose-1,2-enediol-furfural route and D-xylose-D-xylulose-1,2-enediol-furfural route are coexisted under HNO_3 acid catalysis. When using THF as reaction medium, the transformation between D-xylose and D-xylulose are blocked, thus the dominant reaction pathway under H_2SO_4, HNO_3 or HCl acid is D-xylose-1,2-enediol-furfural route.

Similarly, the reaction pathway of D-xylulose-to-furfural conversion can also be divided into two routes: the first one is D-xylulose-1,2-enediol-furfural route; the second one is D-xylulose-D-xylose-1,2-enediol-furfural route. For all tested acids in the solvent of water or THF, the D-xylulose-1,2-enediol route has a much larger reaction rate constant than that of D-xylulose-D-xylose-1,2-enediol route, as shown in Table 3, thus the dominant reaction pathway is D-xylulose-1,2-enediol-furfural route.

3. Conclusion

We have proposed a reaction mechanism for the D-xylose-to-furfural conversion under homogenous acid catalysis, which includes formation of D-xylulose by hydride shift as well as enolization of both D-xylose and D-xylulose. Detailed energetics of the mutual transformations among D-xylose, 1,2-enediol intermediate and D-xylulose over different strong acids were studied with quantum chemistry calculations in different solvents including water and THF. Based on the assumption of 1,2-enediol formation being the rate limiting step, a simplified kinetic model was constructed to describe the D-xylose/D-xylulose-to-furfural conversion in water. The results show a good agreement with the reported experiments, implying that the simplification that furfural is directly generated from the 1,2-enediol by one-step reaction is very reasonable. Based on the energy barriers in the mutual transformation among D-xylose, D-xylulose and 1,2-enediol, the dominant reaction pathways of D-xylose/D-xylulose-to-furfural formation are determined under different acid catalysis when using water or THF as reaction medium.

Declaration of competing interest

The authors declare that they have no known competing financial interests or personal relationships that could have appeared to influence the work reported in this paper.

Acknowledgements

We acknowledge financial support by the National Key R&D Program of China (2019YFC1906700). This article is also funded by China Scholarship Council.

Appendix A. Supplementary data

Supplementary data to this article can be found online at https://doi.org/10.1016/j.carres.2021.108463.

References

[1] G.W. Huber, J.N. Chheda, C.J. Barrett, J.A. Dumesic, Production of liquid alkanes by aqueous-phase processing of biomass-derived carbohydrates, Science 308 (5727) (2005) 1446–1450.
[2] X. Li, P. Jia, T. Wang, Furfural: a promising platform compound for sustainable production of C4 and C5 chemicals, ACS Catal. 6 (11) (2016) 7621–7640.
[3] G.W. Huber, S. Iborra, A. Corma, Synthesis of transportation fuels from biomass: chemistry, catalysts, and engineering, Chem. Rev. 106 (9) (2006) 4044–4098.
[4] M.C. McCann, M.S. Buckeridge, N.C. Carpita, Plants and Bioenergy, Springer, 2014.
[5] O. Ershova, J. Kanervo, S. Hellsten, H. Sixta, The role of xylulose as an intermediate in xylose conversion to furfural: insights via experiments and kinetic modelling, RSC Adv. 5 (82) (2015) 66727–66737.
[6] C.D. Hurd, L.L. Isenhour, Pentose reactions. I. furfural formation, J. Am. Chem. Soc. 54 (1) (1932) 317–330.
[7] M.S. Feather, The conversion of D-xylose and D-glucuronic acid to 2-furaldehyde, Tetrahedron Lett. 11 (48) (1970) 4143–4145.
[8] M.S. Feather, D.W. Harris, S.B. Nichols, Routes of conversion of D-xylose, hexuronic acids, and L-ascorbic acid to 2-furaldehyde, J. Org. Chem. 37 (10) (1972) 1606–1608.
[9] M.J. Antal, T. Leesomboon, W.S. Mok, G.N. Richards, Mechanism of formation of 2-furaldehyde from d-xylose, Carbohydr. Res. 217 (1991) 71–85.
[10] K. Yan, G. Wu, T. Lafleur, C. Jarvis, Production, properties and catalytic hydrogenation of furfural to fuel additives and value-added chemicals, Renew. Sustain. Energy Rev. 38 (2014) 663–676.
[11] M.R. Nimlos, X. Qian, M. Davis, M.E. Himmel, D.K. Johnson, Energetics of xylose decomposition as determined using quantum mechanics modeling, J. Phys. Chem. 110 (42) (2006) 11824–11838.
[12] N.R. Vinueza, E.S. Kim, V.A. Gallardo, N.S. Mosier, M.M. Abu-Omar, N.C. Carpita, et al., Tandem mass spectrometric characterization of the conversion of xylose to furfural, Biomass Bioenergy 74 (2015) 1–5.
[13] W.A. Bonner, M.R. Roth, The conversion of D-Xylose-1-C14 into 2-Furaldehyde-α-C14, J. Am. Chem. Soc. 81 (20) (1959) 5454–5456.
[14] D.W. Harris, M.S. Feather, Evidence for a C-2→C-1 intramolecular hydrogen-transfer during the acid-catalyzed isomerization of D-glucose to D-fructose ag], Carbohydr. Res. 30 (2) (1973) 359–365.
[15] B. Danon, G. Marcotullio, W. de Jong, Mechanistic and kinetic aspects of pentose dehydration towards furfural in aqueous media employing homogeneous catalysis, Green Chem. 16 (1) (2014) 39–54.
[16] J.B. Binder, J.J. Blank, A.V. Cefali, R.T. Raines, Synthesis of furfural from xylose and xylan, ChemSusChem 3 (11) (2010) 1268–1272.
[17] G. Marcotullio, W. De Jong, Furfural formation from d-xylose: the use of different halides in dilute aqueous acidic solutions allows for exceptionally high yields, Carbohydr. Res. 346 (11) (2011) 1291–1293.
[18] G. Marcotullio, W. De Jong, Chloride ions enhance furfural formation from D-xylose in dilute aqueous acidic solutions, Green Chem. 12 (10) (2010) 1739–1746.
[19] M. Frisch, G.W. Trucks, H.B. Schlegel, G.E. Scuseria, M.A. Robb, J.R. Cheeseman, et al., Gaussiañ 09 Revision D. 01, 2014.
[20] M. Wang, C. Liu, Q. Li, X. Xu, Theoretical insight into the conversion of xylose to furfural in the gas phase and water, J. Mol. Model. 21 (11) (2015) 296.
[21] L. Yang, G. Tsilomelekis, S. Caratzoulas, D.G. Vlachos, Mechanism of brønsted acid-catalyzed glucose dehydration, ChemSusChem 8 (8) (2015) 1334–1341.
[22] Y. Zhang, C. Liu, X. Chen, Mechanism of glucose conversion in supercritical water by DFT study, J. Anal. Appl. Pyrol. 119 (2016) 199–207.
[23] E.A. Pidko, V. Degirmenci, E.J.M. Hensen, 9, On the Mechanism of Lewis Acid Catalyzed Glucose Transformations in Ionic Liquids, vol. 4, 2012, pp. 1263–1271.
[24] X. Huang, D-g Cheng, F. Chen, X. Zhan, Reaction pathways of hemicellulose and mechanism of biomass pyrolysis in hydrogen plasma: a density functional theory study, Renew. Energy 96 (2016) 490–497.
[25] L. Negureanu, R.W. Hall, L.G. Butler, L.A. Simeral, Methylaluminoxane (MAO) polymerization mechanism and kinetic model from Ab initio molecular dynamics and electronic structure calculations, J. Am. Chem. Soc. 128 (51) (2006) 16816–16826.
[26] A.E. Keating, S.R. Merrigan, D.A. Singleton, K.N. Houk, Experimental proof of the non-least-motion cycloadditions of dichlorocarbene to Alkenes:kinetic isotope effects and quantum mechanical transition states, J. Am. Chem. Soc. 121 (16) (1999) 3933–3938.
[27] P. Brandt, C. Hedberg, P.G. Andersson, New mechanistic insights into the iridium–phosphanooxazoline-catalyzed hydrogenation of unfunctionalized olefins, A DFT Kinetic Stud. 9 (1) (2003) 339–347.
[28] H. Farrokhpour, M. Manassir, Approach for predicting the standard free energy solvation of H+ and acidity constant in nonaqueous organic solvents, J. Chem. Eng. Data 59 (11) (2014) 3555–3564.
[29] F. Parveen, S. Upadhyayula, Efficient conversion of glucose to HMF using organocatalysts with dual acidic and basic functionalities-A mechanistic and experimental study, Fuel Process. Technol. 162 (2017) 30–36.
[30] M.P. Andersson, P. Uvdal, New scale factors for harmonic vibrational frequencies using the B3LYP density functional method with the triple-ζ basis set 6-311+G(d,p), J. Phys. Chem. 109 (12) (2005) 2937–2941.
[31] B.P. Pritchard, D. Altarawy, B. Didier, T.D. Gibson, T.L. Windus, New basis set exchange: an open, up-to-date resource for the molecular sciences community, J. Chem. Inf. Model. 59 (11) (2019) 4814–4820.

[32] K.L. Schuchardt, B.T. Didier, T. Elsethagen, L. Sun, V. Gurumoorthi, J. Chase, et al., Basis set exchange:A community database for computational sciences, J. Chem. Inf. Model. 47 (3) (2007) 1045–1052.
[33] C.P. Kelly, C.J. Cramer, D.G. Truhlar, Aqueous solvation free energies of ions and ion– water clusters based on an accurate value for the absolute aqueous solvation free energy of the proton, J. Phys. Chem. B 110 (32) (2006) 16066–16081.
[34] M.J. McGrath, I.W. Kuo, J.N. Ghogomu, C.J. Mundy, A.V. Marenich, C.J. Cramer, et al., Calculation of the Gibbs free energy of solvation and dissociation of HCl in water via Monte Carlo simulations and continuum solvation models, Phys. Chem. Chem. Phys. 15 (32) (2013) 13578–13585.
[35] A. Trummal, L. Lipping, I. Kaljurand, I.A. Koppel, I. Leito, Acidity of strong acids in water and dimethyl sulfoxide, J. Phys. Chem. 120 (20) (2016) 3663–3669.
[36] R.P. Bell, The Proton in Chemistry, Springer Science & Business Media, 2013.
[37] T. Ahmad, L. Kenne, K. Olsson, O. Theander, The formation of 2-furaldehyde and formic acid from pentoses in slightly acidic deuterium oxide studied by 1H NMR spectroscopy, Carbohydr. Res. 276 (2) (1995) 309–320.
[38] S. Dutta, S. De, B. Saha, M.I. Alam, Advances in conversion of hemicellulosic biomass to furfural and upgrading to biofuels, Catalys. Sci. Technol. 2 (10) (2012) 2025–2036.
[39] I. Agirrezabal-Telleria, I. Gandarias, P. Arias, Heterogeneous acid-catalysts for the production of furan-derived compounds (furfural and hydroxymethylfurfural) from renewable carbohydrates: a review, Catal. Today 234 (2014) 42–58.
[40] O. Yemiş, G. Mazza, Acid-catalyzed conversion of xylose, xylan and straw into furfural by microwave-assisted reaction, Bioresour. Technol. 102 (15) (2011) 7371–7378.
[41] K.J. Zeitsch, The Chemistry and Technology of Furfural and its Many By-Products, Elsevier, 2000.
[42] X. Fang, Z. Wang, W. Song, S. Li, W. Lin, Preparation of furans from catalytic conversion of corn stover in H2O–THF co-solvent system–The effects of acids combined with alkali metal cations, J. Taiwan Inst. Chem. Eng. 97 (2019) 105–111.
[43] V. Choudhary, S.I. Sandler, D.G. Vlachos, Conversion of xylose to furfural using Lewis and Brønsted acid catalysts in aqueous media, ACS Catal. 2 (9) (2012) 2022–2028.
[44] A.A. Rosatella, S.P. Simeonov, R.F. Frade, C.A. Afonso, 5-Hydroxymethylfurfural (HMF) as a building block platform: biological properties, synthesis and synthetic applications, Green Chem. 13 (4) (2011) 754–793.
[45] X. Qi, M. Watanabe, T.M. Aida, R.L. Smith Jr., Catalytical conversion of fructose and glucose into 5-hydroxymethylfurfural in hot compressed water by microwave heating, Catal. Commun. 9 (13) (2008) 2244–2249.
[46] Y. Román-Leshkov, J.A. Dumesic, Solvent effects on fructose dehydration to 5-hydroxymethylfurfural in biphasic systems saturated with inorganic salts, Top. Catal. 52 (3) (2009) 297–303.
[47] N. Shi, Q. Liu, Q. Zhang, T. Wang, L. Ma, High yield production of 5-hydroxymethylfurfural from cellulose by high concentration of sulfates in biphasic system, Green Chem. 15 (7) (2013) 1967–1974.
[48] C.M. Cai, T. Zhang, R. Kumar, C.E. Wyman, THF co-solvent enhances hydrocarbon fuel precursor yields from lignocellulosic biomass, Green Chem. 15 (11) (2013) 3140–3145.
[49] L. Zhang, H. Yu, P. Wang, Y. Li, Production of furfural from xylose, xylan and corncob in gamma-valerolactone using FeCl3· 6H2O as catalyst, Bioresour. Technol. 151 (2014) 355–360.
[50] X. Li, Q. Liu, C. Luo, X. Gu, L. Lu, X. Lu, Kinetics of furfural production from corn cob in γ-valerolactone using dilute sulfuric acid as catalyst, ACS Sustain. Chem. Eng. 5 (10) (2017) 8587–8593.